SPECIAL CRITERIA DEVELOPED FOR THE DESIGN AND ANALYSIS OF FLOATING NUCLEAR PLANT CONTAINMENT STRUCTURES

J. C. TSAI, R. S. ORR

Offshore Power Systems
8000 Arlington Expressway, Jacksonville, Florida 32211, U.S.A.

SUMMARY

Offshore Power Systems (OPS) is designing and manufacturing standardized Floating Nuclear Plants (FNP). The plant utilizes an ice-condenser and dual containment system with a free-standing steel shell welded to the upper deck of the steel platform. The pressure retaining portion of the platform upper deck in the containment area is designated as the containment baseplate. Certain unique loadings and configurations dictate the development of special criteria for the design and analysis of containment and other safety-related structures. Three topics of these special criteria are presented herein.

1. Containment Shell Buckling Criteria. — Non-uniform internal pressure transients during LOCA result in a dynamic shell response having significant compressive zones which govern the shell buckling design. The shell has longitudinal and circumferential stiffening for increased buckling capacity. In the shell analyses, finite element computer programs are first used to obtain stress resultants based on linear dynamic shell response to pressure transients. These stress resultants are then compared against buckling allowables established from linear shell buckling analyses reduced by factors which reflect the difference between theoretical and design buckling capacities of the shell. Factors affecting shell buckling design include shell and stiffener configurations, combined effects of longitudinal, circumferential and tangential shear load components, gross and local shell buckling, geometric imperfections (based on Koiter's theory), dynamic loading, boundary effects including those due to platform deformation, and overall safety factors. Results of buckling analyses using sample cases are presented.

2. Containment Baseplate Design Criteria. — The containment baseplate consists of flat plate panels stiffened with girders and stiffeners. It serves both as part of the platform and lower boundary of the containment vessel. All transverse loadings acting on the baseplate are transmitted to the platform bulkheads supporting the baseplate. Following a review of both ASME and AISC Codes, design criteria were developed based on the ASME Code Subsection NE criteria for flat heads supplemented by built-up I-section and orthotropic deck considerations. These criteria which utilize the stress intensity approach and ultimate capacity of design sections were found to be better suited for the design of containment vessel pressure barriers than other code criteria such as those dealing with linear type components.

3. Criteria for Missile Impact on Steel Panels. — Due to weight and manufacturing considerations, steel panels are used in many locations as missile barriers as compared with the concrete barriers widely used on land-based plants. Current empirical formulas for evaluating required thicknesses for steel missile barriers are not totally applicable to the characteristics of missiles encountered in nuclear power plant design. OPS is sponsoring test programs for small scale and full scale missile impact tests on steel panels. These programs are designed to provide new insight into missile impact phenomena including scale laws and provide guidelines for steel missile barrier design. Results of nine small scale tests and one full scale test are presented. The full scale test was a 12″ pipe impacting a steel panel at 210 fps.

1.0 INTRODUCTION

Offshore Power Systems (OPS) is currently designing standardized floating nuclear plants (FNPs) to be manufactured in a shipyard-type facility in Jacksonville. In 1984, the first unit will be towed from the manufacturing facility and delivered to a site off the coast of New Jersey prepared by the Public Service Electric and Gas Company. The concept of standardized floating nuclear plants and their manufacturing in a central facility is described in Ref. [1].

The FNP utilizes a PWR ice-condenser containment system with a free-standing steel containment vessel surrounded by a reinforced concrete shield building (Fig. 1). The containment vessel houses the three major compartments of the ice condenser containment system, namely, the lower compartment, the ice condenser compartment, and the upper compartment. An annular space between the vessel and the shield building together with the space beneath the vessel in the leak-tight compartments of the platform provides a secondary containment barrier for control of leakage.

All containment structures are attached to the top deck of the floating platform (Fig. 2) which serves as the foundation for the plant. The platform is an all-welded steel structure approximately 400 feet long, 378 feet wide and 44 feet deep with full depth bulkheads in both longitudinal and transverse directions extending the length and width of the platform to form a grid. Additional framing is provided between bulkheads at the top deck, bottom shell and sides with deep girders in line with vertical webs in the transverse direction and stiffeners in the longitudinal direction. Inner bottoms similar to the top deck or bottom shell are provided in many compartments to serve as part of watertight or leak-tight barriers.

The containment vessel consists of the steel containment shell and the steel containment base plate. The containment base plate is the pressure retaining portion of the platform top deck in the containment area. This and other types of unique configurations as well as loadings associated with the floating nuclear plant concept dictated the development of special criteria for the design and analysis of containment and other safety-related structures. Of these special criteria, the development of three criteria is discussed in this paper.

2.0 CONTAINMENT SHELL BUCKLING CRITERIA

2.1 Description

The containment shell is a free-standing welded steel structure with a 124 foot high vertical cylinder and a torispherical dome roof. It is welded at the cylinder base to the containment base plate. The inside diameter of the cylinder is 120 feet and the crown of the dome roof rises about 35 feet above the spring line. The three major compartments of the ice condenser containment system inside the containment vessel are divided into further sub-compartments by walls and floors of the interior structure and major equipment. In the event of a postulated loss-of-coolant accident, the ice condenser condenses the steam and reduces the pressure load substantially below that experienced by a dry containment. The flow of air and steam through sub-compartments creates non-uniform transient pressures which act dynamically on the containment vessel and interior structures with variable intensity and distribution. Significant analytical effort is required to define structural responses under this type of loading.

2.2 Shell Response to Transient Pressures

The dynamic response of the containment shell to a typical ice condenser containment non-uniform internal transient pressures indicates a pattern of wave-like response of the shell in both the longitudinal and circumferential directions with dynamic amplification occurring at the first few impulses of the pressure transients. This regional response giverns the majority of the shell design in terms of both the stress and buckling effects. A finite element axisymmetric shell program [2] and a three dimensional finite element computer program [3] were used to define and verify the shell response to transient pressures.

2.3 Stress Intensity Design

The containment shell is designed to the rules of NE-3000 of the ASME Code [4]. For class MC components, the ASME Code uses the stress intensity approach which is based on the Tresca yield criterion. In determining the required shell thicknesses for the containment shell, stress resultants from elastic dynamic analysis of the shell subject to transient pressures were combined with stress resultants due to other design loadings to define the maximum stress intensity values in each zone of the shell. The required shell thicknesses are selected such that these maximum stress intensity values do not exceed the allowables specified in NE-3000.

2.4 Shell Stability Design

In addition to the stress intensity limits, the containment shell must also satisfy the stability stress limits of NE-3000; however, for determining the critical buckling stresses of the shell, NE-3000 only provides general guidelines. Thus, specific buckling criteria were developed by OPS based on these guidelines with the assistance of Professors T. P. Kicher of Case Western Reserve University, Cleveland, Ohio and C. D. Babcock of California Institute of Technology, Pasadena, California. These criteria are based on the classical linear bifurcation analysis reduced by margins which reflect the difference between theoretical and actual load capacities of the shell. The bifurcation point is defined as the point at which two equilibrium paths intersect.

The maximum thickness of the main shell plates was limited to 1.5 inches to preclude the necessity for postweld heat treatment. This limitation plus parametric studies between stiffened and unstiffened shell led to the use of longitudinal and circumferential stiffening for the cylindrical part of the shell. The circumferential stiffeners are 1" x 18" ring plates generally spaced at 10 foot centers, while the longitudinal stiffeners are 1" x 6" flat bars spaced at 3° angular intervals. The latter spacing was chosen to make the shell panel between stiffeners behave more like a flat plate than a shell segment based on criteria established in Ref. [5].

2.4.1 Classical Buckling Surface

The classical linear bifurcation analysis has long been the basis for theoretical buckling analysis of shell type structures as well as other type structures. This classical approach establishes the bifurcation load analytically for a perfect shell model under the combined buckling effects of longitudinal compression (or tension), circumferential compression (or tension) and in-plane shear. The bifurcation loads for different combinations of buckling load components thus obtained define an envelope of buckling capacities for the perfect shell model under various loading conditions. Several computer programs available in the public domain can define this envelope fairly consistently given the same geometry, boundary conditions and loading conditions. The computer programs used by OPS were specifically developed to analyze efficiently the types of shell to be used (cylindrical and torispherical, stiffened or unstiffened) under combined longitudinal, circumferential and shear loads. Gross and local buckling behaviors of shell segments or shell panels can be analyzed by these programs to define the critical buckling loads.

2.4.2 Capacity Reduction (Knock-Down) Factors

It has been demonstrated through extensive experimental programs that theoretical linear bifurcation analysis predicts buckling loads exceeding those observed experimentally. For example, an unstiffened cylindrical shell subjected to axial compression exhibits severe deviations while similar deviations but to a lesser degree were observed for shell structures subjected to circumferential compression or in-plane shear. These deviations are attributed to the presence of initial imperfections which precipitate premature buckling because they preclude the pure membrane state and provide a lower energy response path to the buckled state. The presence of imperfections furthermore changes the buckling character from one of linear bifurcation to one of a limit point on the non-linear equilibrium path. Further investigations have established that the capacity reductions of structures due to imperfections are closely related to the post buckling response curves. Structures where the post buckling curve suffers no drop after bifurcation will not be susceptible to the detrimental effects of imperfections. A good example of this is the buckling behavior of flat plates with proper edge supports. Stiffened shells are also generally less sensitive to imperfections than an equivalent unstiffened shell and consequently, exhibit closer correlation between analysis and experiment. The ASME Code incorporates the above concept of capacity reduction due to imperfections in the containment vessel design and specifies the imperfections as maximum deviations from true theoretical form in NE-4000.

Based on a literature search of published analytical results and test data, some sample knock-down curves due to imperfections for cylindrical shells under axial compression, external pressure and torsion load are given in Figs. 3, 4 and 5, respectively. It can be noticed that significant spread of curves exists in all three figures. However, when one bears in mind that these curves are obtained from different sources which cover buckling analyses of widely different structures, then the spread is understandable and the ranges of spread can be considered as reasonable.

To do a full scale knock-down analysis from the classical buckling surface for combined load components requires a very sophisticated computer analysis supplemented by the use of engineering judgement in the analytical process. Therefore, it is not practical to use this as the main tool in the containment vessel buckling design. In the absence of such analysis or large scale test programs, a simple and conservative approximation using knock-down factors for each load component based on Koiter's theory [6, 7, 8, 9] can be employed. This method compares favorably with other similar analytical or empirical methods yet provides a consistent approach to the problems related to the imperfection sensitivity analysis of structures.

In actual application of this method in a buckling design, it is more convenient to increase each load component of the combined buckling loads artifically by dividing each load component with its respective knock-down factor. Each load component is further increased by the required overall safety factor. These increased load components represent a single load vector which is then compared against the classical buckling surface for the particular shell segment under consideration. If all load vectors thus obtained stay within the classical buckling surface, then the shell segment is considered to be properly designed.

2.4.3 Dynamic Criteria of Shell Stability

Structures which are sensitive to imperfection may suffer a further loss in buckling load capacity if the loads are applied dynamically. The presence of imperfections and multiple response paths due to the interaction of the modes of deformation allow the structure to change from the fundamental state of deformation to a buckled state at a lower load level. The static buckling loads can be corrected for effects of dynamic loads as described below when the effects of imperfection are properly characterized.

Results of studies presented in Refs. [10, 11, 12] incidate that for cylindrical shells under dynamically applied step loadings, the smallest ratio of dynamic buckling load capacity to the static buckling load capacity is 0.71 for lateral or hydrostatic (external) pressure if the imperfections are small (amplitude less than half the shell thickness); and 0.54 for axial compression after many cycles of response using initial imperfection values taken from experimental models. The dynamic buckling load referred to in these studies represents the magnitude of the applied step load. The response of the shell to this loading based on a linear transient analysis would show a dynamic load factor of about two on the stresses over the same loading applied statically. There is, therefore, no reduction in buckling capacity due to dynamic loading when the evaluation of static buckling capacity is based on the peak stresses in the shell determined from a linear transient analysis.

3.0 CONTAINMENT BASE PLATE DESIGN CRITERIA

The containment base plate consists of the top deck of the platform inside the shield building and the bulkheads and innerbottom surrounding the in-core instrumentation sump below the top deck. It serves both as part of the platform and as the lower boundary of the containment vessel. The base plate, together with the girders and stiffeners welded to it, transmits all of its loadings to the platform bulkheads supporting the base plate.

In addition to the platform stress criteria (which are not covered in this paper), the base plate must also meet the stress criteria related to the pressure boundary of a containment vessel. NE-3000 of the ASME Code [4] does not provide in specific detail rules for the design of stiffened flat heads for containment vessels, thus design criteria needed to be developed to assure a safe design of all details of the base plate. Code Case 1733 recently adopted by the ASME Committee provides some guidelines to the design of structural members other than solid rectangular sections; however, it is still not comprehensive in details as to be used solely as the base plate design criteria.

In developing the design criteria for the base plate, a number of existing codes have been reviewed. Among them are the American Bureau of Shipping (ABS) Rules for Steel Vessels, the American Institute of Steel Construction (AISC) Design Manual for orthotropic bridge decks, and other criteria for linear type components such as the AISC Specification for building structures and Subsection NF of the ASME Code. Based on considerations regarding material, design, fabrication, and above all the compatibility with the containment shell as parts of the containment vessel, the ASME Code Subsection NE criteria for flat heads supplemented by the built-up section and orthotropic deck considerations were chosen as the basis for developing the base plate design criteria.

The stress intensity criteria of the ASME Code for primary membrane plus primary bending stresses are based on the collapse stresses of solid rectangular sections under combined loadings (Fig. 6). For a rectangular section, the collapse stress (in terms of the yield stress) for combined tension (or compression) and bending is defined as the ratio of the pseudo-elastic stress intensity representing the full plastic capacity of the section divided by the stress intensity producing initial yielding in the extreme fibers of the section. In calculating the full plastic capacity of the section, the stress-strain relationship of an elastic or rigid-perfectly plastic material is assumed. From collapse stresses for different combinations of membrane and bending stresses, an envelope can be defined. This envelope reduced by safety factors is used as the basis for establishing design limits. For simplicity, the ASME Code replaces the curved envelope for rectangular sections with a constant factor of 1.5.

The same design philosophy used in developing the ASME stress intensity criteria is also used to develop the base plate design criteria. For a built-up non-rectangular section under combined membrane and bending loads, a similar envelope of collapse stresses can be defined for various combinations of membrane and bending stresses (Fig. 6). This envelope reduced by the same safety factors of the ASME Code becomes the basis for establishing design limits for the non-rectangular section. One significant difference between the non-rectangular section and the rectangular section is that the envelope varies among different non-rectangular sections depending on shapes of section and loading patterns. Thus, to use a conservatively low constant factor to represent all envelopes of non-rectangular sections in establishing the design limits may turn out to be too conservative for some design applications.

In a stiffened flat plate construction, if the stiffening in one direction is much heavier than the other direction, the structure behaves more like a series of beam-type or one-way-slab type members rather than two-way-plate type members. For the former type members, appropriate stress intensity criteria need to be established for stresses at gross structural discontinuities to ensure adequate safety factors against the overall collapse of any structural member. For typical structural members in the containment base plate, our study has shown that at gross structural discontinuities stress intensity allowables equal to 133% of that allowed in general areas for primary membrane plus primary bending will provide adequate safety margins.

One additional effect associated with the stiffened construction which needs to be considered is the shear lag effect. This effect is the local stress increase or decrease in a built-up non-rectangular section due to in-plane shear deformation of a plate element when its width-thickness ratio becomes large. This local stress increase is similar to the local primary membrane stress increase in a vessel design due to loads acting on penetration sleeves or bracket attachments. An increase of 50% in stress intensity allowables as specified in the base plate design criteria for this local effect is consistent with the ASME design approach.

4.0 CRITERIA FOR MISSILE IMPACT ON STEEL PANELS

Due to weight and manufacturing considerations of the FNP, steel panels are used in many locations as missile barriers (mainly for external missiles) rather than the concrete barriers widely used on land-based nuclear plants. For the same structural strength, a steel structure is generally lighter in weight as compared to a concrete structure, and is also more amenable to shop fabrication and large field subassemblies. To manufacture the FNPs under assembly line conditions and specifically to utilize the 900 metric ton gantry crane at the manufacturing facility effectively, structures are designed as much as practicable into modules and large subassemblies. Concrete structures are used mainly in areas where radiation shielding is required.

For evaluation of required thickness for steel missile barriers, current industry practice is to follow empirical formulae established from early test programs such as the Stanford Research Institute (SRI) formula [17] or the Ballistic Research Laboratories (BRL) formula [17]. These formulae are applicable within the ranges of parameters covered by the test programs. To apply these formulae for missile and target characteristics outside the applicable ranges requires engineering judgement or supplemental test programs. OPS initiated small scale and full scale tests of missile impact on steel panels at different research institutes to verify the adequacy of applying these formulae to the design of FNP steel missile barriers. The test programs are continuing. Although the tests are oriented toward external missile barrier design, with data analysis, test results should be equally applicable to the design of internal missile barriers having similar missile impact characteristics. Two small scale tests by Southwest Research Institute of San Antonio, Texas and one full scale test by Calspan Corporation of Buffalo, New York are described in this paper.

The specified missile for the three tests was a schedule 40, 12" steel pipe weighing 743 lb. impacting the target panel end-on at 210 fps. The specified target panel (Fig. 7) was 3/4" thick, 9' x 9'-4", steel plate backed up vertically by a WT 18 x 85 section and horizontally by two WT 6 x 7 sections. Behind the horizontal edges of the plate were 4 x 3 x 5/8 angles and behind the vertical edges of the plate were MC 18 x 85 channels. The full scale test panel was supported on a test frame belonging to H. H. Robertson Company [18] and its 16" O.D. launcher was also used in the test. The impact point was specified to be as close as possible to the flanges of a WT 6 x 7 section and the WT 18 x 85 section without the missile being over these flanges. The small scale tests used a scale factor of approximately 1/16 of the full scale and included a test on a 5/8" thick plate as well as the 3/4" plate. In the three actual tests, all test parameters stayed within achievable test accuracies.

Before the two small scale tests, six preliminary small scale tests were performed to do a parametric study of failure mechanisms and effects of plate thicknesses, support conditions, and small panel fabrication techniques. After the two tests, another small scale panel of the 3/4" plate was subjected to a wooden dowel test representing a 13.5" diameter utility pole weighing 1500 lb. and impacting the panel at 210 fps. It was found that the utility pole missile was less critical than the 12" pipe missile.

The full scale test resulted in panel perforation (Fig. 8) with the panel absorbing about 86% of the impact energy. A post-impact material study of the A36 panel steel which included Charpy V-Notch tests of panel specimens (Fig. 9) and scanning electron microscope examinations of fracture surfaces revealed a partial brittle failure. This plus other data analyses of test results suggest a modified SRI formula for steel pipe missile, which correlates the test data of the two small scale and the full scale tests quite well. In the modified formula, a new factor is included which reflects the reduction of the panel energy absorption capacity when the panel is impacted at temperature below its ductile-brittle transition temperature. Test programs are continuing which will investigate this capacity reduction more fully. Figures 10 and 11 show comparisons of panel deformation profiles of the three tests. The modified SRI formula based on preliminary results is given below in a non-dimensional form which can be used for any self consistent set of units

$$\frac{E - E_r}{K\sigma_u d_o h^2} = 4.128 + 0.0967 \frac{W_e}{h}$$

Where E = the projectile impact kinetic energy.

E_r = the projectile residual kinetic energy.

K = target energy absorption capacity reduction factor with respect to its ductile-brittle transition temperature.

σ_u = ultimate tensile strength of the target.

h = target thickness

d = $d_o \left(\frac{4-(h/h_o)^2}{3}\right)\left(\frac{h_o}{h}\right)$

h_o = threshold thickness (incipient perforation)

d_o = projectile outer diameter.

W_e = $1/2\ (r_1 + r_2 + r_3 + r_4)$

r_1 = distance from center of impact to beam or column support edge.

r_2 or r_3 = 2.7d representing effective crater radius for the light stiffener support edge.

r_4 = 3.6d representing full effective crater radius

5.0 CONCLUSIONS

The FNP concept presents some unique challenges for the design and analysis of containment and other safety-related structures. The three examples of criteria development discussed in this paper demonstrate that by following basic design philosophies and extending the design approaches of existing rules and industry practices, the FNP structures can be designed to a high safety level consistent with that of land-based nuclear plants.

REFERENCES

[1] Orr, R. S., Dotson, C., "Offshore Nuclear Power Plants," Nuclear Engineering and Design 25 (1973), 334-349.

[2] Ghosh, S., Wilson, E., "Dynamic Stress Analysis of Axisymmetric Structure under Arbitrary Loading," University of California, Berkely, Earthquake Engineering Research Center Report No. 69-10.

[3] Desalvo, G. J., Swanson, J. A., "ANSYS," Swanson Analysis Systems, Inc., Elizabeth, Pennsylvania.

[4] ASME Boiler and Pressure Vessel Code, Section III - Division I, Nuclear Power Plant Components, Subsection NE, Class MC Components.

[5] Koiter, W. T., "Buckling and Post Buckling Behavior of a Cylindrical Panel under Axial Compression," Report S. 476, National Aero, Research Institute of Amsterdam, Reports and Transactions, Vol. XX, pp. 71-84, 1955.

[6] Koiter, W. T., "On the Stability of Elastic Equilibrium," Ph.D. Thesis, Delft, 1945, Transaction AFFDL-TR-70-25, February, 1970.

[7] Hutchinson, J. W., Amazigo, J. C., "Imperfect Sensitivity of Eccentrically Stiffened Cylindrical Shells," AIAA Journal, Vol. 5, No. 3, pp. 392-401, 1967.

[8] Budiansky, B., Amazigo, J. C., "Initial Post Buckling Behavior of Cylindrical Shells under External Pressure," J. Math. and Phys. Vol. 47, pp. 223-235, 1968.

[9] Budiansky, B., "Post Buckling Behavior of Cylinders in Torsion," Theory of Thin Shells, Springer-Verlag, pp. 212-233, 1969.

[10] Budiansky, B., "Dynamic Buckling of Elastic Structures: Criteria and Estimates," Proc. of the Int. Conference on Dynamic Stability of Structures, pp. 83-106, 1965.

[11] Lockhart, D., Amazigo, J. C., "Dynamic Buckling of Externally Pressurized Imperfect Cylindrical Shells," ASME Journal of Applied Mechanics, June 1975, pp. 316-320.

[12] Tamura, Y. S., Babcock, C. D., "Dynamic Stability of Cylindrical Shells under Step Loading," ASME Journal of Applied Mechanics, Paper No. 75-APMW-17.

[13] Tennyson, R. C., Muggeridge, D. B., Caswell, R.D., "New Design Criteria for Predicting Buckling of Cylindrical Shells under Axial Compression," AIAA Paper No. 71-145, AIAA 9th Aerospace Sciences Meeting, 1971.

[14] Loo, Tsu-Tao, "Effects of Large Deflections and Imperfections on the Elastic Buckling of Cylinders under Torsion and Axial Compression," Proc. of the 2nd U.S. National Congress of Applied Mechanics, pp. 345-357, 1954.

[15] Sobey, A. J., "The Buckling of an Axially Loaded Circular Cylinder with Initial Imperfections," Aeronautical Research Council, R. & M. No. 3430, London, 1966.

[16] Donnell, L. H., "Effect of Imperfections of Buckling on Thin Cylinders under External Pressure," ASME J. Applied Mechanics, Vol. 23, pp. 569-575, 1956.

[17] Gwaltney, R. C., "Missile Generation and Protection in Light-Water-Cooled Power Reactor Plants," Oak Ridge National Lab. (ORNL) NSIC-22, Oak Ridge, Tennessee, 1968.

[18] Ting, R.M.L., "Non-Composite and Composite Steel Panels for Tornado Missile Barrier Walls," 2nd ASCE Spec. Conference on Structural Design of Nuclear Plant Facilities, Session IV, New Orleans, Louisiana, 1975.

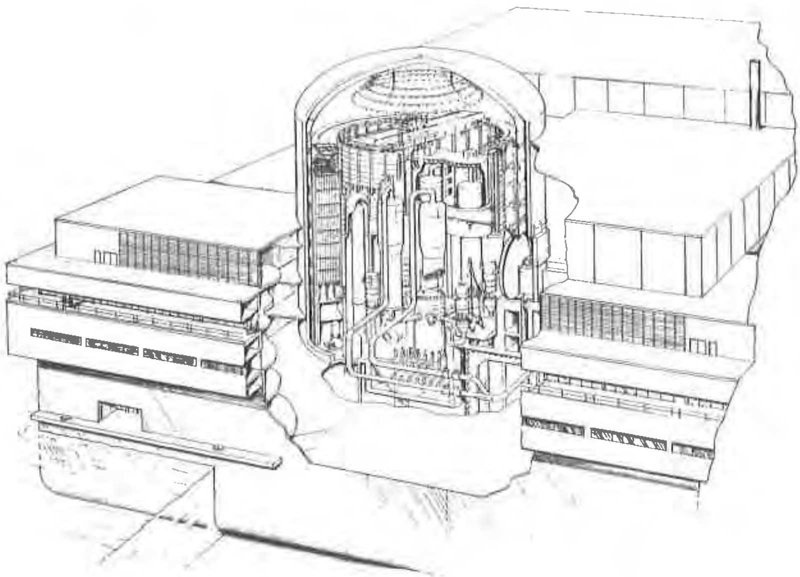

Figure 1 - Cutaway of Containment Building

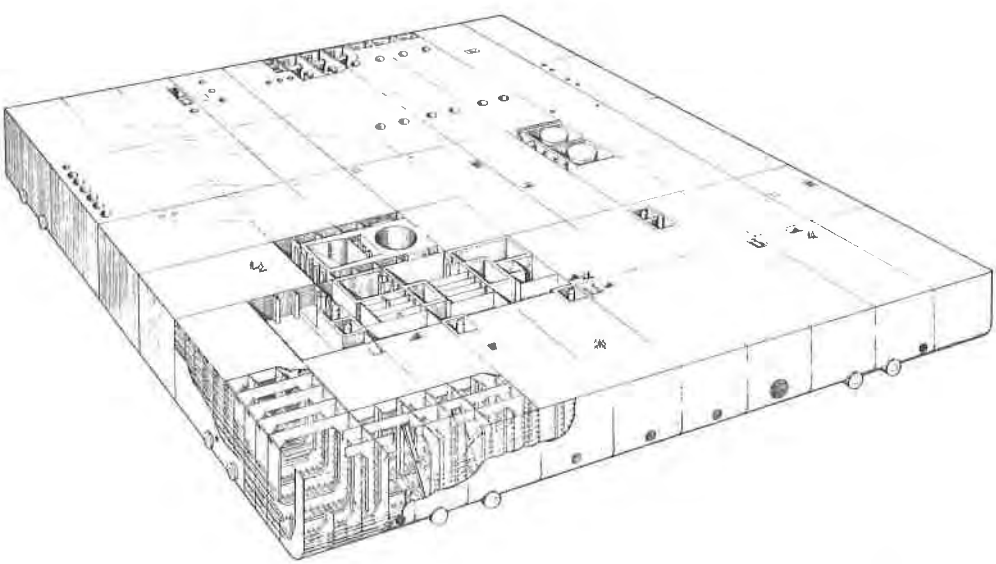

Figure 2 - Platform Structure and Compartmentation

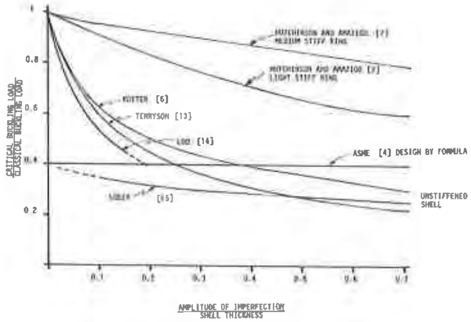

Figure 3 - Effects of Imperfections on the Buckling of Cylindrical Shells under Axial Compression

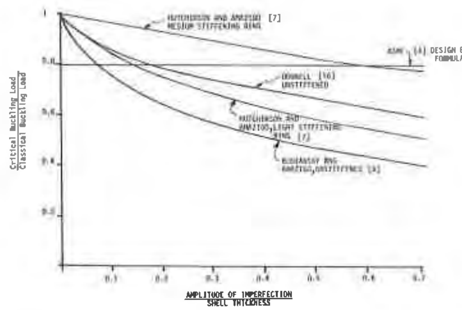

Figure 4 - Effects of Imperfections on the Buckling of Cylindrical Shells under External Pressure

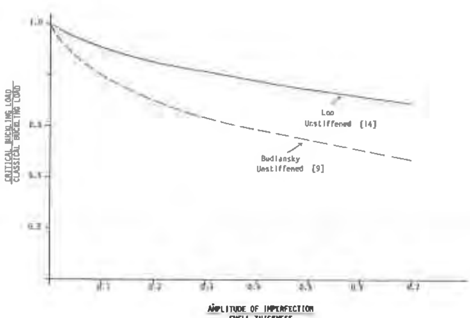

Figure 5 - Effects of Imperfections on the Buckling of Cylindrical Shells under Torsion Load

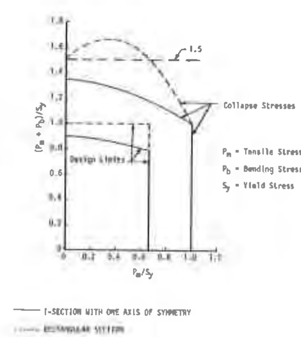

Figure 6 - Collapse Stresses and Design Limits for Combined Tension and Bending

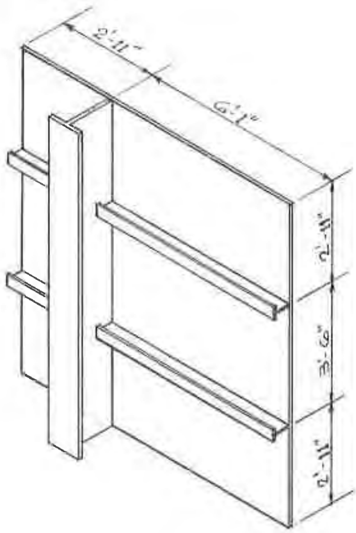

Figure 7 - Back Face Isometric View of Target Panel

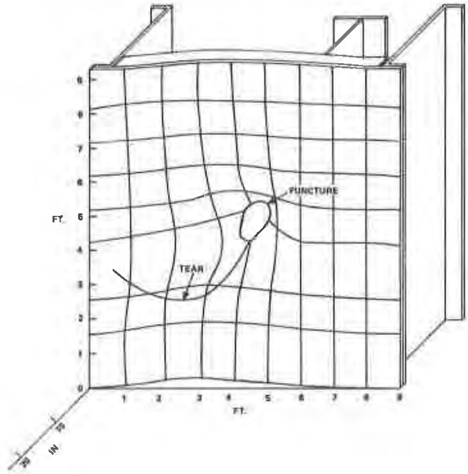

Figure 8 - Three-Dimensional Representation of Post-Test Wall Contour

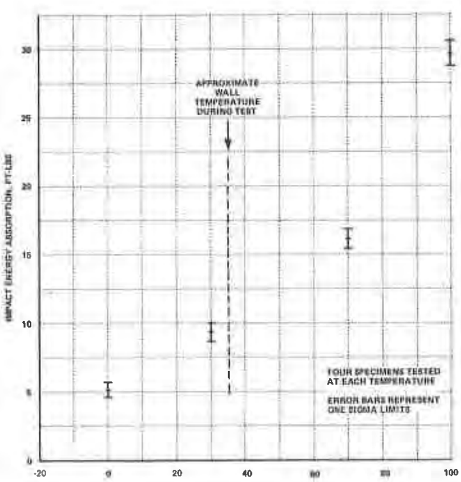

Figure 9 - Charpy V-Notch Test Results

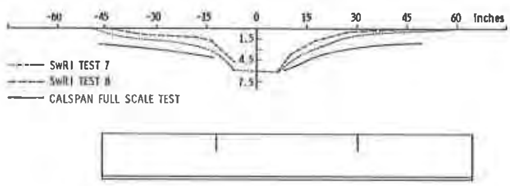

Figure 10 - Comparison of Panel Deformation Profiles (Vertical)

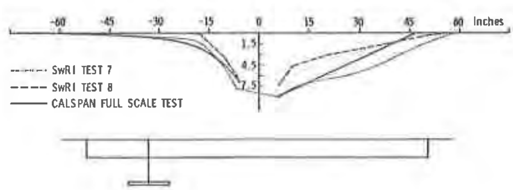

Figure 11 - Comparison of Panel Deformation Profiles (Horizontal)